 

PACS numbers: 42.55.Lt; 34.50.Gb; 52.40.Mj
DOI: 10.1070/QE2011v041n02ABEH014387

# Enhanced technique for measuring collisional quenching rate coefficients in rare-gas mixtures

D.A. Zayarnyi, A.Yu. L'dov, I.V. Kholin

***Abstract*. We set forth an improved technique for the investigation of collisional quenching in high-pressure rare-gas mixtures, which relies on the absorption probing measurements of the decay rates of the excited states of these gases in the afterglow of a fast electron beam discharge. We determined more precisely the rate coefficients of the plasmochemical reactions $Xe^* + Xe + Ar \rightarrow Xe_2^*$ and $Xe^* + Ar \rightarrow$ products $+ Ar$ for the metastable $(6s[3/2]_2^o)$ and resonance $(6s[3/2]_1^o)$ levels of atomic Xe investigated in our earlier work. The rate coefficients for the reactions $Xe(6s[3/2]_2^o) + 2Ar \rightarrow ArXe^* + Ar$ ($(7.2 \pm 1.4) \times 10^{-36}$ cm$^6$ s$^{-1}$) and $Xe(6s[3/2]_1^o) + 2Ar \rightarrow ArXe^*$ ($(5.3 \pm 2.4) \times 10^{-36}$ cm$^6$ s$^{-1}$) were measured for the first time.**

***Keywords***: *rare gases, xenon, argon, excimers, plasmochemistry, collisional quenching, absorption spectroscopy*.

## 1. Introduction

Our work is a continuation of a series of experimental investigations (see review Refs [1, 2] as well as Refs [3, 4]) into the collisional quenching of excited atoms of heavy rare gases in low-lying states in collisions with unexcited atoms of the working and buffer (lighter) gases. These investigations pertain to fundamental areas of physics and at the same time are of paramount practical significance both for high-power near-IR lasers harnessing dense rare-gas mixtures (see review Ref. [5] and references therein) and for high-power UV excimer lasers [6, 7], as well as for other important applications involving the development of high-power compact excimer UV radiation sources [8], television plasma panels [9], etc.

The aim of the present work is to improve the absorption probing technique applied in Refs [1, 2] in an effort to raise the accuracy of measurements of the rate coefficients of plasmochemical reactions responsible for the collisional quenching of the low-lying 6s levels of atomic Xe in Ar – Xe mixtures. We investigated practically important high-pressure Ar – Xe mixtures with low relative Xe densities excited by a fast electron beam. In these mixtures the 6s states of atomic Xe are deexcited in three- and two-particle collisional reactions

$$Xe^* + Xe + Ar \rightarrow Xe_2^* + Ar, \quad (1)$$

$$Xe^* + 2Ar \rightarrow ArXe^* + Ar, \quad (2)$$

$$Xe^* + Ar \rightarrow \text{products} + Ar. \quad (3)$$

When determining the rate coefficient of reaction (3) it is well to bear in mind that the experimentally obtained value is an upper estimate, because account should also be taken of the collisions of excited xenon with atoms and molecules of impurities M in the gas mixture under investigation (primarily impurities in Ar):

$$Xe^* + M \rightarrow \text{products}. \quad (4)$$

Although the densities of different impurities in purified argon are relatively low (see below), the contribution of such reactions may be significant because of their high cross sections.

The reaction rate coefficients were measured by absorption probing technique from the dependences of the 6s-state decay time on the pressure and the working-to-buffer gas density ratio. For this purpose, in the afterglow of a high-power fast electron discharge we investigated the dynamics of probe pulse absorption at wavelengths corresponding to optical transitions with a high oscillator strength between the 6s levels under study and the higher-lying 6p levels (Table 1 and fig. 1).

**Table 1.** Parameters of atomic Xe transitions under investigation.

| Transition | $\lambda/\mu$m | Oscillator strength/$10^{-6}$ s$^{-1}$ |
|---|---|---|
| $6p[1/2]_1 - 6s[3/2]_2^o$ | 0.9800 | 28 |
| $6p[5/2]_3 - 6s[3/2]_2^o$ | 0.8819 | 30 |
| $6p[5/2]_2 - 6s[3/2]_1^o$ | 0.9923 | 16 |
| $6p[1/2]_0 - 6s[3/2]_1^o$ | 0.8280 | 33 |

The excitation of Ar – Xe mixtures by a fast electron beam results in the ionisation and excitation of atoms (primarily of the Ar buffer gas). At high pressures, in the chains of plasmochemical reactions of the types

$$Ar^+ + 2Ar \rightarrow Ar_2^+ + Ar, \quad (5)$$

$$Ar_2^+ + Xe \rightarrow Xe^+ + 2Ar, \quad (6)$$

**D.A. Zayarnyi, A.Yu. L'dov, I.V. Kholin** P.N. Lebedev Physics Institute, Russian Academy of Sciences, Leninsky prosp. 53, 119991 Moscow, Russia; e-mail: kholin@sci.lebedev.ru

Received 5 July 2010
*Kvantovaya Elektronika* **41** (2) 128 – 134 (2011)
Translated by E.N. Ragozin

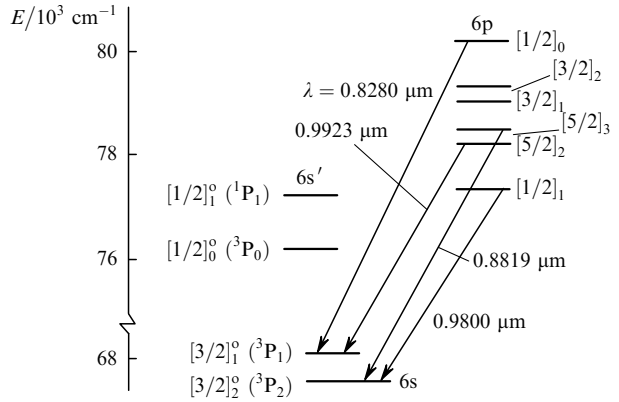


**Figure 1.** Structure of low excited levels of atomic xenon.

$$Xe^+ + Xe(Ar) + Ar \rightarrow Xe_2^+(ArXe^+) + Ar \quad (7)$$

the excitation is transferred to molecular xenon ions. The dissociative recombination of these ions with electrons,

$$Xe_2^+(ArXe^+) + e \rightarrow Xe^{**} + Xe(Ar), \quad (8)$$

leads to the production of xenon atoms in different highly excited states. Then, these states relax rapidly due to collisions with heavy particles and electrons as well as due to the radiative decay to the low excited 6s states of atomic Xe.

In the afterglow of a pulsed electron beam discharge, on completion of recombination and relaxation the densities of the metastable $6s[3/2]_2^o$ state and the resonance $6s[3/2]_1^o$ state (owing to radiation trapping, it may also be treated as a metastable one) investigated in our work are determined primarily by their decay in reactions (1)–(4):

$$\frac{d[Xe^*]}{dt} = -k_1[Xe][Ar][Xe^*] - k_2[Ar]^2[Xe^*]$$

$$-(k_3 + k_4 m)[Ar][Xe^*], \quad (9)$$

where $k_1$ and $k_2$ are the excimerisation rate coefficients in reactions (1) and (2), respectively; $k_3$ is the rate coefficient for two-particle relaxation (3); $k_4$ is the rate coefficient for quenching by impurities in reaction (4); and $m$ is the relative content of impurity M in the mixture under investigation. In this case, the temporal run of the populations of the states under discussion may be represented in the form of an exponential dependence

$$[Xe^*](t) = N_0 \exp(-tk_d) \quad (10)$$

with the quenching rate

$$k_d = k_1[Xe][Ar] + k_2[Ar]^2 + (k_3 + k_4 m)[Ar]. \quad (11)$$

When probing the excited medium by monochromatic radiation at the wavelength of the transition from a highly excited state to the state under investigation, the absorption coefficient $k$ is proportional to the density of atoms in the excited state:

$$k(t) \sim [Xe(6s)](t). \quad (12)$$

In accordance with Bouguer–Lambert–Beer law, the measured transmission coefficient $T$ is related to the absorption coefficient $k$ as

$$\ln(T^{-1}) = kL, \quad (13)$$

where $L$ is the length of the domain under excitation. On taking the logarithm of expression (13), in view of relation (12) and the expected, according to Eqn (10), dependence [Xe(6s)]($t$), we arrive at the following expression for the time dependence of the transmission coefficient $T$ in the afterglow:

$$\ln\ln[1/T(t)] = \text{const} - k_d t. \quad (14)$$

Within the limits of experimental error, the values of $\ln\ln[1/T(t)]$ obtained in the experiments of Refs [1, 2], which were aimed at the measurement of the rate coefficients of reactions (1)–(3), did lie along straight lines. Subsequently [3, 4], the use of digital equipment in the measurement channels enabled the measurement accuracy to be significantly improved. In this case, in our present experiments, like in Refs [3, 4], we could observe an appreciable departure of the experimental dependence $\ln\ln[1/T(t)]$ from a linear one. In Refs [3, 4] this was due to the effect of recombination, when collisional quenching takes place against the background of recombination population of the atomic states under investigation. In the present work, the wavelengths of transitions (Table 1, Fig. 1) suited for absorption measurements fell into the broad absorption bands of one or other of excimer states [10]. In this case, there occurred two different situations. When two short-wavelength transitions ($6p[5/2]_3 - 6s[3/2]_2^o$ and $6p[1/2]_0 - 6s[3/2]_1^o$) were employed for the measurements, the quenching rates $k_d$ obtained for the atomic states involved were lower than excimer decay rates (Fig. 2a). When use was made of two long-wavelength transitions ($6p[1/2]_1 - 6s[3/2]_2^o$ and $6p[5/2]_2 - 6s[3/2]_1^o$), the resultant quenching rates were higher than excimer decay rates (Fig. 2b). As we shall see subsequently, in the linear approximation of the experimental dependences $\ln\ln[1/T(t)]$ in the former case there would be an overestimation and in the latter case (these transitions were previously unexplored) an underestimation of the measured rates in comparison with the real collisional quenching rates. The methods of correct determination of excited-state decay rates in the case of absorption measurements in broad absorption bands will be considered in our future work. The aim of the present work is to elaborate a technique of processing experimental signals that would permit, by way of adequate approximation of the curve $\ln\ln[1/T(t)]$, separating the collisional quenching of excited Xe atoms from the quenching of excimers recorded from broadband absorption, and thereby permit improving the accuracy of determination of the quenching rate coefficients for the metastable,

$$Xe(6s[3/2]_2^o) + Xe + Ar \rightarrow Xe_2^* + Ar, \quad (15)$$

$$Xe(6s[3/2]_2^o) + 2Ar \rightarrow ArXe^* + Ar, \quad (16)$$

$$Xe(6s[3/2]_2^o) + Ar \rightarrow \text{products} + Ar, \quad (17)$$

and resonance,

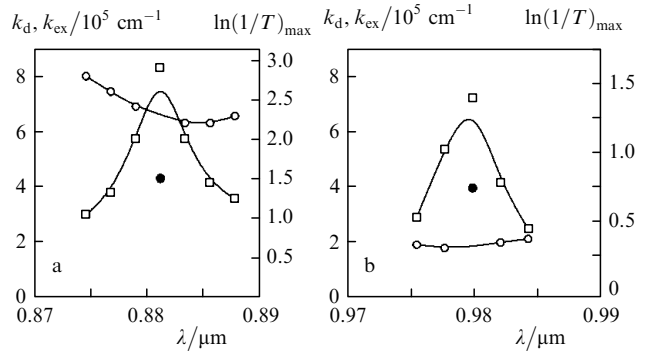


**Figure 2.** Decay rates of excited states of xenon and excimers $k_d$ (●) and $k_{ex}$(○), as well as amplitudes (□) of absorption pulses obtained from the data of absorption measurements in the vicinity of transitions $6p[5/2]_3 - 6s[3/2]_2^o$ (a) and $6p[1/2]_1 - 6s[3/2]_2^o$ (b) of atomic Xe for an Ar:Xe = 200:1 mixture at a pressure of 3.0 atm.

$$Xe(6s[3/2]_1^o) + Xe + Ar \rightarrow Xe_2^* + Ar, \quad (18)$$

$$Xe(6s[3/2]_1^o) + 2Ar \rightarrow ArXe^* + Ar, \quad (19)$$

$$Xe(6s[3/2]_1^o) + Ar \rightarrow Xe(6s[3/2]_2^o) + Ar, \quad (20)$$

levels of atomic Xe (Table 2).

**Table 2.** Collisional quenching rate coefficients $k_i$ for the states $6s[3/2]_2^o$ and $6s[3/2]_1^o$ of Xe atoms in an Ar–Xe mixture.

| Reaction | Rate coefficient | Reference |
|---|---|---|
| (15) | $2.3 \times 10^{-32}$ cm$^6$ s$^{-1}$ | [11] |
| | $(2.15 \pm 0.25) \times 10^{-32}$ cm$^6$ s$^{-1}$ | [12] |
| | $2.6 \times 10^{-32}$ cm$^6$ s$^{-1}$ | [13] |
| | $(1.5 \pm 0.2) \times 10^{-31}$ cm$^6$ s$^{-1}$ | [14] |
| | $(1.8 \pm 0.6) \times 10^{-32}$ cm$^6$ s$^{-1}$ | [2] |
| | $(6.79 \pm 0.68) \times 10^{-33}$ cm$^6$ s$^{-1}$ | Present work |
| (16) | $(3 \pm 3) \times 10^{-34}$ cm$^6$ s$^{-1}$ | [15] |
| | $< 10^{-35}$ cm$^6$ s$^{-1}$ | [2] |
| | $(7.2 \pm 1.4) \times 10^{-36}$ cm$^6$ s$^{-1}$ | Present work |
| (17) | $(8.3 \pm 1.5) \times 10^{-17}$ cm$^3$ s$^{-1}$ | [12] |
| | $(5.0 \pm 0.7) \times 10^{-16}$ cm$^3$ s$^{-1}$ | [15] |
| | $(7.3 \pm 0.9) \times 10^{-16}$ cm$^3$ s$^{-1}$ | [14] |
| | $(2.5 \pm 0.8) \times 10^{-15}$ cm$^3$ s$^{-1}$* | [16] |
| | $(2.80 \pm 0.28) \times 10^{-15}$ cm$^3$ s$^{-1}$ | Present work |
| (18) | $(2.1 \pm 0.2) \times 10^{-31}$ cm$^6$ s$^{-1}$ | [12] |
| | $4.5 \times 10^{-32}$ cm$^6$ s$^{-1}$ | [13] |
| | $(8.6 \pm 0.4) \times 10^{-32}$ cm$^6$ s$^{-1}$ | [14] |
| | $(2.8 \pm 0.9) \times 10^{-32}$ cm$^6$ s$^{-1}$ | [2] |
| | $(2.00 \pm 0.20) \times 10^{-32}$ cm$^6$ s$^{-1}$ | Present work |
| (19) | $< 10^{-35}$ cm$^6$ s$^{-1}$ | [2] |
| | $(5.3 \pm 2.4) \times 10^{-36}$ cm$^6$ s$^{-1}$ | Present work |
| (20) | $(1.5 \pm 0.3) \times 10^{-14}$ cm$^3$ s$^{-1}$ | [12] |
| | $1.7 \times 10^{-14}$ cm$^3$ s$^{-1}$ | [17] |
| | $3.0 \times 10^{-14}$ cm$^3$ s$^{-1}$ | [13] |
| | $(4.0 \pm 0.5) \times 10^{-13}$ cm$^3$ s$^{-1}$ | [18] |
| | $(3.2 \pm 1.5) \times 10^{-15}$ cm$^3$ s$^{-1}$ | [2] |
| | $(3.27 \pm 0.33) \times 10^{-15}$ cm$^3$ s$^{-1}$ | Present work |

* This value of the rate coefficient of reaction (17) was borrowed from original work [16], because there was a misprint in review Ref. [2].

## 2. Experimental facility

Experiments were executed on a Tandem pulsed laser facility with a cold-cathode electron gun (for more details, see Ref. [19]). A pulsed ~ 250-keV electron beam of section 5 × 100 cm with a bell-shaped current envelope and a base duration of ~ 2.5 μs was introduced into the measuring chamber perpendicular to its optical axis through 20-μm thick titanium foil. The electron current density was equal to 1.5 A cm$^{-2}$. The measuring chamber with an active volume of 5 L was made of stainless steel. Prior to gas puffing it was evacuated to a residual pressure of ~ $10^{-5}$ Torr via a liquid nitrogen trap; the inleakage of air to the chamber did not exceed $10^{-3}$ Torr h$^{-1}$. We investigated the mixtures of high-purity argon (99.998 % pure) with high-purity xenon (99.9992 % pure) with component ratios Ar:Xe = 300:1, 200:1, 100:1, and 50:1 at a pressure of 1–4 atm.

Figure 3 is a schematic of the optical measurement scheme. An ISI-1 broadband light source (*1*) with a pulse duration of ~ 30 μs served as the source of probe radiation. At the output of the source the radiation was collimated to a beam 5 cm in diameter and, on transit through the measurement chamber (*5*) with the mixture under investigation, was focused onto the entrance slit of an MDR-2 high-transmission monochromator (*8*) with a 600 line mm$^{-1}$ diffraction grating as the dispersing element. The radiation transmitted through the monochromator, which was tuned to a wavelength under investigation (see Table 1), was focused onto photodetector (*10*). The photodetector comprised a BPW34 (Infinion) fast-response pin-photodiode and an AD8055 (Analog Devices) wideband operational amplifier, which were accommodated in a double-screened metal case. To suppress the short-wavelength radiation in the second diffraction order, a KS-10 light filter (*3*) was placed into the probe beam at the output of the ISI-1 source. A part of the radiation was reflected from a plane-parallel glass plate (*4*), which was located in front of the measurement chamber, and was directed past the chamber to a DMR-4 monochromator (*9*), which was tuned to the same wavelength as the MDR-2 monochromator, and to the second photodetector (*11*). The signals from the photodetectors were recorded by a DSO-2010 (Link Instruments) two-channel digital oscilloscope connected to a computer. The oscilloscope, the computer, and an autonomous accumulator power supply were accommodated in a screening metal rack. This measurement scheme enabled us to simultaneously record the shape and amplitude of the

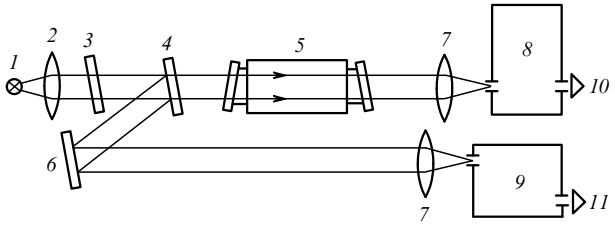


**Figure 3.** Optical schematic of absorption measurements: (*1*) ISI-1 pulsed light source; (*2*) collimating lens; (*3*) KS-10 light filter; (*4*) beamsplitting plate; (*5*) measurement chamber; (*6*) deflecting mirror; (*7*) focusing lenses; (*8*) MDR-2 high-transmission monochromator; (*9*) DMR-4 monochromator; (*10*), (*11*) photodetectors.

probing pulse with a temporal resolution of better than 100 ns before to and after the absorption medium.

The scheme shown is the result of amendment of the measurement scheme involving the sequential recording of the light pulses transmitted through the excited and unexcited mixtures under investigation, which was employed in Refs [1, 2] earlier. The previous technique limited the accuracy of absorption measurements because of the inability to provide sufficiently high pulse-to-pulse reproducibility of the ISI-1 radiation source [Fig. 4, curve (*2*)]. This was due to the fact that the characteristics of the high-voltage air discharge in the channel of a dielectric plate, which is employed to produce visible radiation in the ISI-1 pulsed radiation source, depend heavily on the diameter and other physical characteristics, which vary from pulse to pulse because of the gradual channel damage by the electric discharge. Going over to the two-channel measurement scheme with simultaneous recording of the signals at the input and output of the cell with the gas mixture under investigation allowed us to solve this problem.

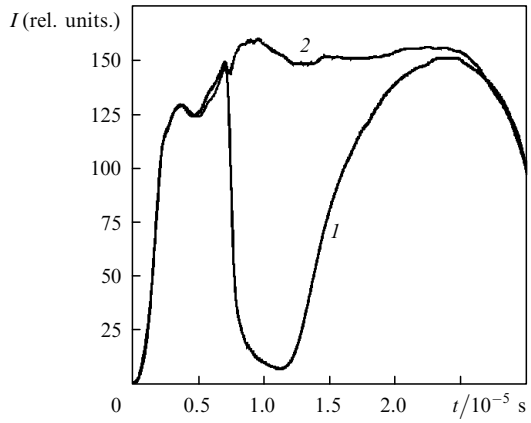


**Figure 4.** Time dependences of the signals from ISI-1 at $\lambda = 0.8819$ μm (the $6p[5/2]_3 - 6s[3/2]_2^o$ transition) transmitted through the excited volume (*1*) and gone past it (*2*). The mixture is Ar:Xe = 200:1 at a pressure of 3.5 atm.

The photodetectors employed in the experiment also underwent modernisation. In this case, the use of fast-response wide-aperture BPW34 photodiodes simplified the alignment of the measurement scheme for obtaining the optimal signal on the oscilloscope screen. Accommodating the preamplifier and the accumulator power supply directly in the metal casing of the photodetector allowed us to obtain the requisite signal-to-noise ratio under intense electromagnetic interference during the operation of the Tandem facility. Furthermore, the low output resistance of the preamplifier allowed matching the photodetectors to the 50-ohm inputs of the oscilloscope, which improved the frequency characteristics of the measurement setup without a sacrifice in sensitivity. Lastly, use was made of the modern digital recording scheme, which simplified the procedure of recorded-signal processing and enhanced its accuracy.

## 3. Measurements on transitions with wavelengths of 0.8819 and 0.8280 μm

Figure 4 depicts the characteristic oscilloscope traces of the probing radiation pulse from the ISI-1 source obtained for the metastable $6s[3/2]_2^o$ level on the $6p[5/2]_3 - 6s[3/2]_2^o$ transition with $\lambda = 0.8819$ μm. By comparing the signals at the input [curve (*2*)] and the output [curve (*1*)] of the excited active medium it is possible to determine the transmission coefficient $T$ of the medium under investigation at each point in time at the wavelength the monochromator is set to. For the oscilloscope traces depicted in Fig. 4, Fig. 5 shows the time dependences of the absorption and the quantity $\ln\ln(1/T)$ for the trailing edge of the absorption pulse.

As noted above, it turned out that the temporal run of the quantity $\ln\ln(1/T)$ was different from the linear one for the $\lambda = 0.8819$- and 0.8280-μm transitions, the experimental dependences $\ln\ln[1/T(t)]$ (see, for instance, Fig. 5b) for all mixtures and pressures investigated had the appearance of an upward concave curve. When the monochromator was set to wavelengths longer or shorter than the atomic transition wavelengths by a value exceeding the instrument function of the monochromator, the amplitude of absorption pulse broadly flattened out (Fig. 2a). In this case, the time dependence $\ln\ln[1/T(t)]$ became linear, with the gradient of slope somewhat stronger than the gradient of slope of the initial portion of the curve in Fig. 5b.

In the processing of the trailing edges of absorption pulses it should be borne in mind that in our case, when the entrance and output slit widths ($\sim 0.2$ mm) of the MDR-2

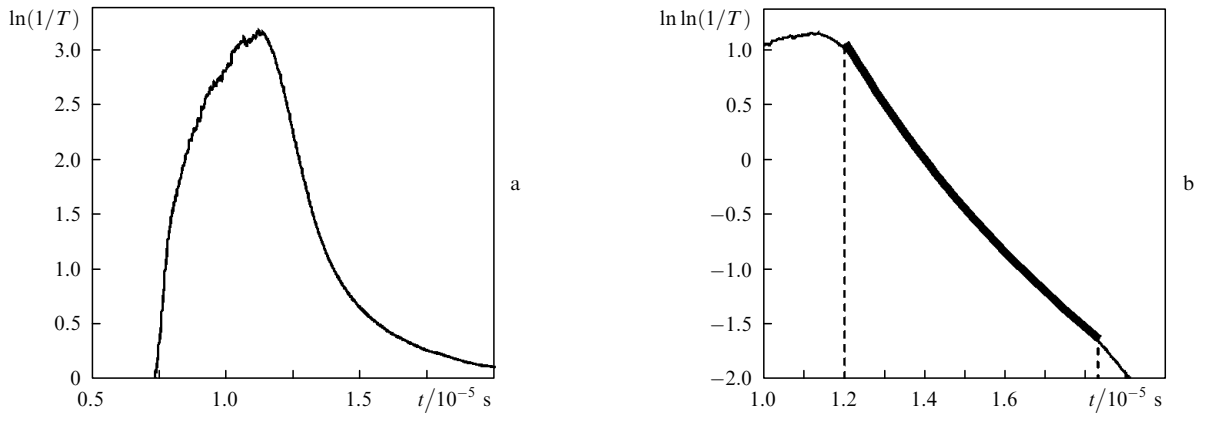


**Figure 5.** Time dependences of absorption (a) and the quantity $\ln\ln(1/T)$ approximated by the curve $\ln[p_d \exp(-\gamma k_d t) + p_{ex} \exp(-k_{ex} t)]$ (the bold curve) (b) for the signals plotted in Fig. 4.

monochromator provide a satisfactory signal-to-noise ratio in the measurement path, the halfwidth of the instrument function of the monochromator in the pressure range (1.0–4.0 atm) under investigation is much greater than the halfwidth of the lines arising from the optical transitions under study. In this situation the Bouguer–Lambert–Beer law, generally speaking, does not hold and use has to be made of the empirical, or the so-called modified form of the Bouguer–Lambert–Beer law [20, 21], which relates the measured transmission coefficient $T$ to the absorption coefficient $k$ by the equation

$$\ln(T^{-1}) = (kL)^{\gamma}. \tag{21}$$

Here, $\gamma$ is a dimensionless factor, which assumes values in the range 1.0–0.5, depending on the ratio between the halfwidths of the absorption line and the instrument function of the monochromator. An examination of experimental dependences

$$\ln\ln[1/T(L)] = \text{const} - \gamma\ln(kL) \tag{22}$$

(for more details, see Ref. [22]) showed that the modified Bouguer–Lambert–Beer law was applicable under our conditions and permitted us to evaluate the dimensionless factor $\gamma$ at 0.5 for all four atomic transitions under study. Therefore, expression (14) should be rearranged to give

$$\ln\ln[1/T(t)] = \text{const} - \gamma k_{\text{d}} t. \tag{23}$$

In this case, in the broadband absorption range, where the Bouguer–Lambert–Beer law should be obeyed, the measured value of $\gamma$ did turn out to be equal to unity.

In view of the aforesaid, it would be natural that the processing of experimental signals would be performed by approximating the trailing edges of absorption pulses (Fig. 5a) by a superposition of two exponential curves,

$$\ln(1/T) = p_{\text{ex}}\exp[-k_{\text{ex}}(t-t_0)] + p_{\text{d}}\exp[-\gamma k_{\text{d}}(t-t_0)], \tag{24}$$

or by the expression

$$\ln\ln(1/T) = \ln\{p_{\text{ex}}\exp[-k_{\text{ex}}(t-t_0)] + p_{\text{d}}\exp[-\gamma k_{\text{d}}(t-t_0)]\} \tag{25}$$

in the coordinates of Fig. 5b, with four variable parameters: $p_{\text{ex}}$, $k_{\text{ex}}$, $p_{\text{d}}$, $k_{\text{d}}$. In this case, the second, 'slower' exponential function $p_{\text{d}}\exp[-\gamma k_{\text{d}}(t-t_0)]$ is defined by the reactions of collisional quenching of the atomic Xe 6s levels under study with the sought-for rates $k_{\text{d}}$. The first, 'faster' exponential function $p_{\text{ex}}\exp[-k_{\text{ex}}(t-t_0)]$ arises from the superposition of the processes under investigation and the absorption of the probing signal by excimer molecules decaying with rates $k_{\text{ex}}$.

The quenching rates were calculated from experimental dependences in Fig. 5b by least squares technique with variation of the $p_{\text{d}}$, $k_{\text{d}}$, $p_{\text{ex}}$, and $k_{\text{ex}}$ coefficients and the use of the Levenberg–Marquardt algorithm. The calculations were made for the experimental data set for mixtures with Ar:Xe = 50:1, 100:1, and 200:1 component ratios at a pressure $p = 1.25 - 4$ atm for the $6s[3/2]_2^o$ level and for Ar:Xe = 100:1, 200:1, and 300:1 mixtures for a pressure $p = 1.0 - 3.0$ atm for the $6s[3/2]_1^o$ level with steps of 0.25 atm.

The description of the trailing edges of absorption pulses outlined above yields quite satisfactory results in the dynamic range of transmittance measurements $T = 0.1-9$ (see Fig. 4). In particular, Fig. 6 shows the dependence of the quantity $k_{\text{d}}[\text{Ar}]^{-1}$ on the density of the Ar buffer gas for Ar–Xe mixtures of different composition. In this case, in agreement with the expected, according to expression (11), linear form of the dependences

$$k_{\text{d}}[\text{Ar}]^{-1} = (\delta k_1 + k_2)[\text{Ar}] + k_3 + k_4 m \tag{26}$$

($\delta = [\text{Xe}]/[\text{Ar}]$ is the relative content of xenon in the mixture), experimental points do fit nicely into straight lines emanating from a common point on the ordinate axis, which testifies to the adequacy of representation (25) and the correctness of the procedure of experimental data processing as a whole. We also emphasise that the values of $k_{\text{ex}}$ resulting from the above procedure of the processing of the dependences in Fig. 5b were in excellent agreement with the decay rates measured from broadband absorption away from the atomic transition.

The set of experimental values of $k_{\text{d}}^{(i)}$ ([Xe], [Ar]) obtained as indicated above was employed to determine the rate coefficients for plasmochemical reactions (1), (2) and to obtain an upper estimate for the rate of reaction (3),

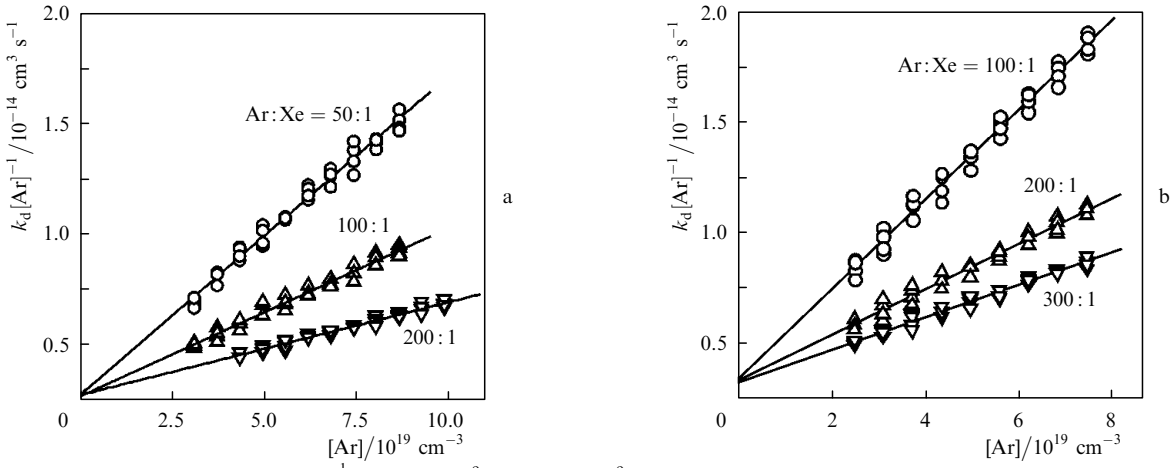


**Figure 6.** Reduced quenching rates $k_{\text{d}}[\text{Ar}]^{-1}$ of the $6s[3/2]_2^o$ (a) and $6s[3/2]_1^o$ (b) levels as functions of argon density in Ar–Xe mixtures of different composition.

correct to the unknown quantity $k_4 m$. The rate coefficients $k_1$, $k_2$, and $k_3$ presented in Table 2 were calculated by the least squares technique with recourse to the Levenberg–Marquardt algorithm and with variation of the sought-for constants in the relations

$$k_{\mathrm{d}}^{(i)} = k_1[\mathrm{Xe}][\mathrm{Ar}] + k_2[\mathrm{Ar}]^2 + k_3[\mathrm{Ar}] \tag{27}$$

simultaneously for the entire set of experimental $k_{\mathrm{d}}^{(i)}$ values. The heart of the procedure reduced to the construction of a curved surface

$$S([\mathrm{Xe}], [\mathrm{Ar}]) = k_1[\mathrm{Xe}][\mathrm{Ar}] + k_2[\mathrm{Ar}]^2 + k_3[\mathrm{Ar}], \tag{28}$$

in the coordinates [Xe], [Ar] that least diverged, in terms of this technique, from the experimental data set (Fig. 7).

It is pertinent to note that the calculated values of the quenching rates $k_{\mathrm{d}}^{(i)}$ for a linear approximation of the dependences $\ln\ln[1/T(t)]$ (see, for instance, Fig. 5b) turn out to be higher than those which result from the above procedure and correspond, to within the experimental error of our measurements, to the values given in our earlier papers (see Table 2).

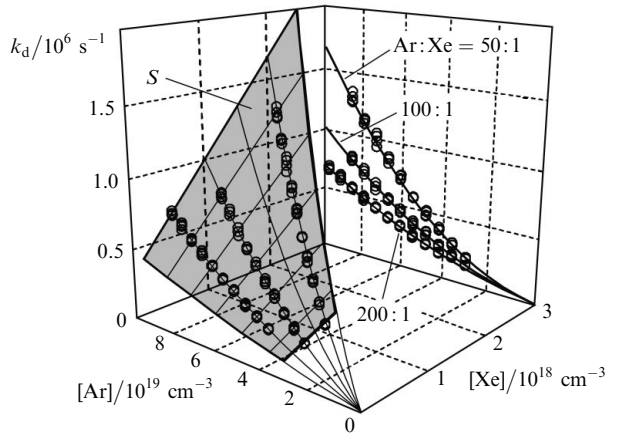


**Figure 7.** Curved surface $S$ ([Xe], [Ar]), which least diverges from the experimental set of points $k_{\mathrm{d}}^{(i)}$ ([Xe], [Ar]) for the $6s[3/2]_2^o$ level, and projection of the resultant three-dimensional image on the plane [Ar], $k_{\mathrm{d}}$ for Ar–Xe mixtures of different composition.

## 4. Measurements on transitions with wavelengths of 0.9800 and 0.9923 μm

The indicated wavelengths are close to the long-wavelength cutoff of the spectral response of our instrumentation and are poorly suited for precision quantitative measurements of collisional quenching rate coefficients for excited states of atomic Xe in an Ar–Xe mixture. We shall nevertheless dwell briefly on the resultant data because of their methodical importance.

Figure 8 shows the temporal dependences of absorption and the value of $\ln\ln(1/T)$ for the trailing edge of absorption pulse, which were obtained for the metastable $6s[3/2]_2^o$ level at a wavelength $\lambda = 0.9800$ μm arising from the $6p[1/2]_1 - 6s[3/2]_2^o$ transition. Like with $\lambda = 0.9923$ μm arising from the $6p[5/2]_2 - 6s[3/2]_1^o$ transition, the experimental dependences $\ln\ln[1/T(t)]$ had a clearly defined convexo-concave shape. By analogy with the dependences obtained in our earlier work on collisional quenching in Ar–Kr mixtures, the convexity in the initial portion of the trailing edge is attributable to the influence of uncompleted recombination processes upon the cessation of a pumping pulse. The existence of a 'slow' tail testifies to the effect of broadband absorption by excimers with a low decay rate, which we detected earlier in the spectroscopic studies of absorption away from atomic transitions (see Fig. 2b). Under these assumptions, the dependences shown in Fig. 8 may be approximated by the formulas

$$\ln(1/T) = p_{\mathrm{d}} \exp\left[-g^2(t-t_0)^2\right] \exp[-\gamma k_{\mathrm{d}}(t-t_0)] + p_{\mathrm{ex}} \exp[-k_{\mathrm{ex}}(t-t_0)], \tag{29}$$

$$\ln\ln(1/T) = \ln\left\{p_{\mathrm{d}} \exp\left[-g^2(t-t_0)^2\right] \exp[-\gamma k_{\mathrm{d}}(t-t_0)] + p_{\mathrm{ex}} \exp[-k_{\mathrm{ex}}(t-t_0)]\right\}, \tag{30}$$

where the first term in expression (29)

$$p_{\mathrm{d}} \exp\left[-g^2(t-t_0)^2\right] \exp[-\gamma k_{\mathrm{d}}(t-t_0)]$$

describes the exponential collisional quenching of the 6s states under study with the Gaussian preexponential factor $\exp[-g^2(t-t_0)^2]$, which takes into account recombination and relaxation processes (see also Refs [3, 4]), while the second, 'slow' term

$$p_{\mathrm{ex}} \exp[-k_{\mathrm{ex}}(t-t_0)]$$

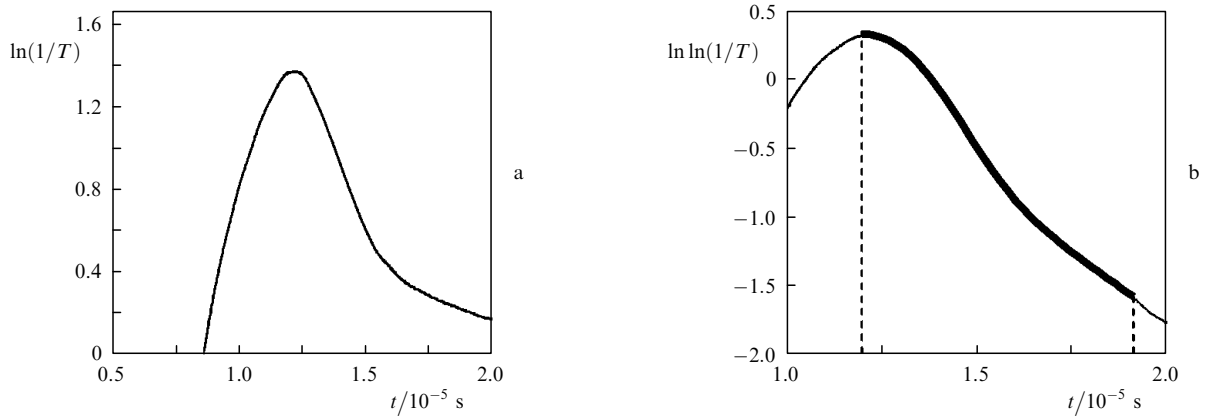


**Figure 8.** Time dependences of absorption (a) and of the value of $\ln\ln(1/T)$ approximated by the curve $\ln\{p_{\mathrm{d}} \exp[-g^2(t-t_0)^2] \exp[-\gamma k_{\mathrm{d}}(t-t_0)] + p_{\mathrm{ex}} \exp[-k_{\mathrm{ex}}(t-t_0)]\}$ (the bold line) (b) at a wavelength $\lambda = 0.9800$ μm (the $6p[1/2]_1 - 6s[3/2]_2^o$ transition). An Ar:Xe = 100:1 mixture at a pressure of 3.5 atm.

takes into account the absorption of probing radiation by excimer molecules.

Like in the previous Section, the 'extraction' of the exponential process of collisional quenching and the calculation of collisional quenching rate coefficients $k_d$ were performed by the least squares technique with recourse to the Levenberg–Marquardt algorithm and with variation of the sought-for constants $p_d$, $k_d$, $p_{ex}$, and $k_{ex}$ in expression (30). In this case, the best result, like in Refs [3, 4], was obtained for the following ratio between the rate coefficients $g$ and $k_d$: $g = 0.6k_d$. We emphasise that the values of quenching rate coefficients $k_d^{(i)}$ calculated by a linear approximation of the dependences $\ln\ln[1/T(t)]$ (see, for instance, Fig. 8b) turn out to be substantially lower than those which result from the procedure described in the foregoing.

In the present work we did the calculations for the set of experimental data measured at a wavelength $\lambda = 0.9800$ μm for mixtures with component ratio Ar:Xe = 100:1 for a pressure $p = 1.25 - 3.5$ atm. Figure 9 shows the dependences of the reduced quenching rate $k_d[\mathrm{Ar}]^{-1}$ on the density of Ar and similar dependences for the shorter-wavelength $6p[1/2]_1 - 6s[3/2]_2^o$ transition with $\lambda = 0.8819$ μm obtained for this mixture. One can see that both dependences coincide to within the experimental error of the measurements, thereby additionally bearing out the correctness of the technique for measuring the rate coefficients for the reactions collected in Table 2.

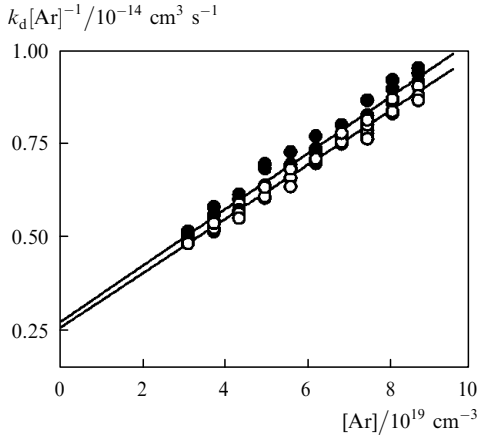


**Figure 9.** Dependences of the reduced quenching rates $k_d[\mathrm{Ar}]^{-1}$ of the $6s[3/2]_2^o$ level on the density of argon, which were obtained from measurements on the $6p[5/2]_3 - 6s[3/2]_2^o$ (●) and $6p[1/2]_1 - 6s[3/2]_2^o$ (○) transitions. Mixture: Ar:Xe = 100:1.

## 5. Conclusions

Our work is primarily methodical in character and is aimed at broadening the potentialities of absorption probing technique in the investigating of collisional quenching in rare-gas mixtures and in prospect of other quenching processes.

The essence of the work done consists in a substantial broadening of the dynamic range and improvement of the signal-to-noise ratio in the measurement path of our facility, in the employment of a two-channel measurement scheme and the change-over to digital measuring instrumentation. All this, combined with the potentialities of the Tandem high-pressure electron-beam facility having a 1-m long active medium and the use of a unique probe radiation source, ISI-1 (Podmoshenskii source), allowed us to achieve a record-high measurement accuracy for the rate coefficients of a number of plasmochemical reactions. In particular, in the experiments described here it has been possible to exceed the accuracy of the heretofore most reliable, in our opinion, measurements, which are summarised in review Ref. [2], and to shorten the confidence interval for the rate coefficients of reactions (15), (17), (18), and (20) to at least 10 %, as well as to measure for the first time the rate coefficients for reactions (16) and (19), which lie in the $10^{-36} - 10^{-35}$-cm$^6$ s$^{-1}$ range and which had admitted only qualitative upper estimates. In Refs [3, 4], which were published slightly earlier and were concerned with the investigation of the reactions of collisional quenching of the 5s level of atomic Kr in Ar–Kr mixtures, we set out the first reliable measurements of the rate coefficients for these reactions, also.

***Acknowledgements.*** In conclusion the authors express their deep gratitude to N.N. Ustinovskii for cooperation and helpful discussions.

## References

1. Zayarnyi D.A., Kholin I.V. *Kvantovaya Elektron.*, **33** (6), 474 (2003) [*Quantum Electron.*, **33** (6), 474 (2003)].
2. Semenova L.V., Ustinovskii N.N., Kholin I.V. *Kvantovaya Elektron.*, **34** (3), 189 (2004) [*Quantum Electron.*, **34** (3), 189 (2004)].
3. Zayarnyi D.A., L'dov A.Yu., Kholin I.V. *Kvantovaya Elektron.*, **39** (9), 821 (2009) [*Quantum Electron.*, **39** (9), 821 (2009)].
4. Zayarnyi D.A., L'dov A.Yu., Kholin I.V. *Kvantovaya Elektron.*, **40** (2), 144 (2010) [*Quantum Electron.*, **40** (2), 144 (2010)].
5. Kholin I.V. *Kvantovaya Elektron.*, **33** (2), 129 (2003) [*Quantum Electron.*, **33** (2), 129 (2003)].
6. Zvorykin V.D., Arlantsev S.V., Bakaev V.G., Gaynutdinov R.V., Levchenko A.O., Molchanov A.G., Sagitov S.I., Sergeev A.P., Sergeev P.B., Stavrovskii D.B., Ustinovskii N.N., Zayarnyi D.A. *J. Phys. IV*, **133**, 567 (2006).
7. Zvereva G.N., Lomaev M.I., Rybka D.V., Tarasenko V.F. *Opt. Spektrosk.*, **102** (1), 36 (2007).
8. Robert E., Sarroukh H., Cachoncinlle C., Viladrosa R., Hochet V., Eddaoui S., Pouvesle J.M. *Pure Appl. Chem.*, **77** (2), 463 (2005).
9. Boeuf J.P. *J. Phys. D: Appl. Phys.*, **36** (6), R53 (2003).
10. Killeen K.P., Eden J.G. *J. Chem. Phys.*, **84** (11), 6048 (1986).
11. Rice J.K., Johnson A.W. *J. Chem. Phys.*, **63** (12), 5235 (1975).
12. Gleason R.E., Bonifild T.D., Keto J.W., Walters G.K. *J. Chem. Phys.*, **66** (4), 1589 (1977).
13. Brunet H., Birot A., Dijols H., Galy J., Millet P., Salamero Y. *J. Phys. B: At. Mol. Opt. Phys.*, **15** (17), 2945 (1982).
14. Sewraj N., Gardou J.P., Salamero Y., Millet P. *Phys. Rev. A*, **62**, 052721 (2000).
15. Kolts J.H., Setser D.W. *J. Chem. Phys.*, **68** (11), 4848 (1978).
16. Sazhina N.N., Ustinovskii N.N., Kholin I.V. *Kvantovaya Elektron.*, **18** (9), 1047 (1991) [*Sov. J. Quantum Electron.*, **21** (9), 949 (1991)].
17. Atzmon R., Cheshnovsky O., Raz B., Jortner J. *Chem. Phys. Lett.*, **29** (3), 310 (1974).
18. Laporte P., Subtil J.L., et al. *Chem. Phys.*, **177** (1), 257 (1993).
19. Zayarnyi D.A., L'dov A.Yu., Kholin I.V. *Prib. Tekh. Eksp.*, (4), 102 (2010).
20. Atzmon R., Cheshnovsky O., Raz B., Jortner J. *Chem. Phys. Lett.*, **29** (3), 310 (1974).
21. Laporte P., Subtil J.L., et al. *Chem. Phys.*, **177** (1), 257 (1993).
22. Zayarnyi D.A., Kholin I.V., Chugunov A.Yu. *Kvantovaya Elektron.*, **22** (3), 233 (1995) [*Quantum Electron.*, **25** (3), 217 (1995)].